SUPPLEMENTAL MATERIAL

Supplemental Methods

Subject recruitment

All subjects were recruited by putting advertisements for healthy volunteers in local New England newspapers. Thereafter, candidates underwent a phone screen to check initial eligibility. The health status of those potential subjects who satisfied the inclusion criteria and did not meet any exclusion criteria, and who were available and willing to undertake a 13 day in-laboratory study was then confirmed by extensive medical history questionnaires followed by electrocardiography, blood chemistry profiles, liver function tests, complete blood count, urinalysis, a history and physical examination (plus a sit-to-stand orthostatic challenge test) by a physician, and a psychiatric and psychological examination by a clinical psychologist. Subjects were excluded if they had history of impaired autonomic function, syncopal attacks, or orthostatic hypotension; or if they were obese (body mass index >30), taking any medications, or had any chronic or current acute medical or psychiatric disease including depression or other psychopathology (e.g., Beck Depression Inventory score $\geq$10 or Minnesota Multiphasic Personality Inventory score $\geq$ 90), hypertension, anemia or other hematologic, hepatic abnormalities; if they reported any current or chronic sleep disturbances or sleep disorders, recent shift work, or circadian rhythm disturbances; if they had a first-degree relative with psychiatric history; or if they reported substance abuse, caffeine dependence (> 4 caffeinated beverages per day), alcohol dependence (> 14 alcoholic drinks per week), or nicotine dependence (> 4 cigarettes per day). Finally, use of all of these substances had to be stopped 3 weeks prior to the start of the inpatient study. To verify these self-reports, a urine sample was tested early in the screening process and at admission to the in-laboratory phase of the study to confirm that the subjects were free from drugs of abuse, alcohol,

caffeine, and nicotine. This recruiting procedure and the study protocol were approved by the local Internal Review Board. All subjects provided informed consent prior to the study.

Circadian analysis

The sleep-wake (or rest-activity) cycle affects core body temperature (CBT) as does the endogenous circadian cycle controlled by the circadian pacemaker[1]. Normally (i.e., outside the laboratory) the sleep-wake cycle and the circadian cycle in humans are 'entrained' with the same period (24 hours), together causing a reduced CBT during sleep at night. In the forced desynchrony (FD) protocol, the two rhythms have different periods, i.e., 20 hours for the imposed behavioral (sleep-wake) cycle and ~24 hours for the endogenous circadian cycle. Thus, the behavioral and circadian rhythms oscillate back and forth between in-phase and out-of-phase states gradually throughout the FD, and the phase relationship between the two rhythms oscillates with a period of 5 days (six 20-hour cycles). For instance, during the first and 7th behavioral cycles, the behavioral cycle and the circadian cycle were in phase (sleep during the biological night), causing a higher amplitude of the overall CBT rhythm (see 0-24 hours and 120-144 hours in **Supplemental Figure I**); and on other days sleeping occurs during (some of) the biological day reducing CBT when the circadian cycle is increasing CBT, resulting in a reduced CBT amplitude. With knowledge of the imposed behavioral cycle (20 hours), the phase, period and amplitude of the underlying circadian CBT rhythm can be statistically estimated by nonlinear least squares regression, which is a standard technique in the circadian field[1]. The components in the regression include multiple sinusoidal waveforms to represent (1) the fundamental and additional 7 harmonics of the 20-hour behavioral cycle (periods = 20, 20/2, 20/3, …, 20/8 hours, respectively), and (2) the fundamental and second harmonics of the circadian rhythm (periods = ~24, ~24/2 hours, respectively). A polynomial trend was also included if there is any significant effect across

all days of the protocol. In the current study, the mean circadian period (the fundamental circadian waveform) was 24.09 h [range 23.8-24.6 h] in these subjects (**Supplemental Figure II**).

Circadian phases are expressed in degrees, with 360º representing the period of the circadian oscillator (~24 h). For each subject, each data point was assigned a circadian phase (between 0^o and 360^o) depending upon the time of the point from the CBT minimum of the fitted circadian waveform (0°) and the subject's estimated circadian period (one full circadian period = 360°) (**Supplemental Figure II**). To assess the circadian rhythms of cardiovascular variables, we performed cosinor analyses in which actual phases for data (instead of 60^o phase bins) were used to yield the cosinor model plots (e.g., see lines on Figure 6 and **Supplemental Figure IV**). In the cosinor analysis of each cardiovascular variable, we included both the fundamental (~24-h) and second harmonics (~12-h) of the endogenous circadian rhythm to allow fitting of a more complex circadian oscillation instead of a simple sinusoidal waveform (see Cosinor analysis using mixed model ANOVA below).

In order to aid understanding and relevance to living outside the laboratory, these circadian phases (0-360º) are also presented as equivalent clock time across the day (0-24 hour). Note, for this calculation, it is necessary to determine the clock time at which the first CBT minimum occurred when entering the lab (**Supplemental Figure II**). Although no binning was used in the cosinor analyses, for visualization purposes and to provide evidence that the model fits the data, it is appropriate to present data points superimposed on the model fit. However, since data were not obtained at every single phase, and since different subjects have data at slightly different phases from each other, the data were averaged into the smallest bin whereby all subjects contribute data to each bin. This optimal bin width for this protocol was 60º, which approximates into ~4 h per bin.

Cosinor analysis using mixed model ANOVA

To assess circadian rhythms, Halberg initially provided a simple cosinor model which fits repeated observations to a fundamental sinusoidal regression function [2]:

$$Y_i = \mu + \alpha \cos(2\pi\, t_i / \tau - \beta) + \varepsilon_i \tag{1}$$

where Y_i is the ith observation (or data point) at time t_i, μ is the mean or MESOR (midline estimating statistic of rhythmicity), τ is the period of the rhythm, α is the amplitude, β is the acrophase, and ε is the residual error. μ, α and β are the three parameters to be determined from the best fit of all data points $\{t_i\ Y_i\}$. This model in Eq. (1) was later extended to incorporate rhythms of multiple periodicities or non-sinusoidal waveforms and to account for random effects [3-5]:

$$Y_i = \mu + \sum_{k=1}^{h} \alpha_k \cos(2\pi\, t_i / \tau_k - \beta_k) + \varepsilon_i \tag{2}$$

where the index k indicates the kth rhythm or harmonic, and h indicates the total number of sinusoidal functions with different periods. The cosinor model is a nonlinear model in the amplitude and acrophase parameters of sinusoidal functions and it can be transformed to a linear regression model:

$$Y_i = \mu + \sum_{k=1}^{h} [a_k f_k(t_i) + b_k g_k(t_i)] + \varepsilon_i \tag{3}$$

where the functions $f_k(t_i) = \cos(2\pi\, t_i / \tau_k)$ and $g_k(t_i) = \sin(2\pi\, t_i / \tau_k)$ represent the transformation, and the original amplitudes and acrophases can be computed from the transformed linear coefficients a_k and b_{k_i} using the following equations:

$$\alpha_i = \sqrt{a_k^2 + b_k^2}\ ; \quad \beta_k = \tan^{-1}(b_k / a_k) \tag{4}$$

To determine whether or not there are significant circadian rhythms of our physiological variables of interest (e.g., SBP, DBP and HR), we adopted and modified the cosinor model as

described in Eq. (3). Instead of using time (t_i) and period (τ_k), we used circadian phase relative to CBT minimum (θ_i) in order to combine data points from different individuals while accounting individual differences in the circadian period (see Supplemental Figure II). To better describe circadian rhythms of non-sinusoidal shapes, we included the fundamental rhythm of ~12 hours and its first harmonic [i.e., *h=2* in Eq. (3)], which are generally sufficient for adequate description of most physiological circadian rhythms. Moreover, we considered additional effects of condition (baseline or tilt), and its interactions with the four circadian terms. Thus, the full cosinor model used in our study can be described by the following equation:

$$\begin{aligned} Y_i = \quad & \mu + a_1\cos(\theta_i) + b_1\sin(\theta_i) + a_2\cos(2\theta_i) + b_2\sin(2\theta_i) + \\ & [c_0 + c_1\cos(\theta_i) + c_2\sin(\theta_i) + c_3\cos(2\theta_i) + c_4\sin(2\theta_i)]^* C + \varepsilon_i \end{aligned} \tag{5}$$

where *C* is the binary variable for condition (baseline or tilt). There are total 10 coefficients in the model (including intercept) to be determined using multiple linear regressions.

To estimate the coefficients in Eq. (5) for each physiological variable, we pooled all data points of all subjects together and performed a mixed model ANOVA using standard least square regression and the restricted maximum likelihood method (JMP 8.0, SAS Institute Inc, North Carolina). In the mixed model, the terms in Eq. (5) (except for ε_i) were included as fixed effects and subject as a random effect for intercept (see Detailed Model information in Table IV). The resultant $p < 0.05$ for either *cosθ* or *sin θ* indicates a significant circadian rhythm of ~24 hours (the lower of the two p values is always reported in the results). Similarly, $p < 0.05$ for either *cos2θ* or *sin2θ* indicates a significant harmonic rhythm (~12 hours). Based on the obtained regression coefficients and their standard errors from the mixed model, we then calculated the phase locations of the overall peak, the overall trough, the peak-to-trough amplitude, and their standard errors.

Supplemental Results

Heart rate variability analysis in the frequency domain

In addition to the heart rate variability (HRV) analysis in the time domain, we performed the HRV analysis in the frequency domain according to the published standards[6]. Briefly, normal-to-normal heart beat intervals (R-R intervals from adjacent EKG waveforms) were re-sampled to 3.41 Hz (1024 points every 300 seconds) using cubic spline fitting; the power spectrum of R-R intervals was obtained in each 2.5-minute window without gaps of data more than 5 seconds; and the average power spectrum was obtained from all 2.5-minute windows at baseline or during tilting for each cycle. Four additional HRV indices are presented (**Supplemental Figures III** and **IV**):

(i) Total spectral power (TP) of heart rate fluctuations at <0.4Hz. It is known that TP is highly correlated to SDNN. Using a simple linear regression, we found a strong association between TP and SDNN ($r = 0.89$, $p < 0.0001$).

(ii) High frequency power (HF: 0.15-0.4 Hz). Log scale of HF (lnHF) is used to ensure a normal distribution. As a parasympathetic marker, lnHF is highly correlated to RMSSD and pNN50 which are also parasympathetic markers. Using data obtained in this study, we confirmed that there were strong associations between lnHF and RMSSD ($r = 0.90$, $p < 0.0001$) and between lnHF and pNN50 ($r = 0.88$, $p < 0.0001$).

(iii) Low frequency power (LF: 0.04-0.15 Hz). Log scale of LF (lnLF) is used to ensure a normal distribution. lnLF is contributed by both sympathetic and parasympathetic nervous activities and, thus, is not considered as a reliable sympathetic or parasympathetic marker.

(iv) Ratio of LF and HF powers (LF/HF). LF/HF generally reflects the balance of sympathetic and parasympathetic activities, i.e., large values indicate relatively strong

sympathetic activity while small values indicate relative strong parasympathetic activity.

Similar to the results of the time-domain HRV analysis, the frequency-domain HRV analysis revealed that heart rate variability (TP) and parasympathetic indices (lnHF) significantly decreased in response to tilt stress for both groups (**Supplemental Figures IIIA** and **IIIB**). We also found that LF/HF increased in response to tilt stress (**Supplemental Figure IIID**). These findings are consistent with the observation that sympathetic nervous activity assessed by plasma epinephrine and norepinephrine levels increased in response to tilt (**Figures 4C** and **4D**). The tilt-induced decrease in TP was smaller in the subjects with presyncope ($P = 0.0008$; **Supplemental Figure IIIA**) and there were no significant group differences in the tilt effects on other frequency-domain HRV indices (**Supplemental Figures III B-III D**). lnLF showed no significant changes in response to tilt except for the trials of presyncope in which lnLF decreased ($P = 0.03$) (**Supplemental Figure IIIC**). Comparing the 21 trials with presyncope and the 51 trials without presyncope within the same 6 presyncopal subjects, only lnHF showed significantly different tilt-induced change, i.e., the decrease of lnHF was greater during the trials with presyncope ($P = 0.003$) (**Supplemental Figure III B**).

TP, lnHF, and lnLF showed significant circadian rhythms (**Supplemental Figure IV**). All these circadian rhythms showed no significant group differences ($P > 0.1$ for all variables). Note that the circadian profile of TP was virtually identical to that of SDNN (**Figure 6F**) and that the circadian profile of lnHF was virtually identically to that of RMSSD (**Figure 6G**), e.g., for all four variables, the peak was at ~40^o at baseline and the valley was at ~240^o during tilt. LF/HF and its response to tilt showed no significant circadian rhythms.

Power spectral analysis of systolic blood pressure

It has been proposed that the low-frequency (LF, 0.04-0.15Hz) oscillations in systolic blood pressure (SBP) can be used a marker to monitor changes of sympathetic activity[7-9] though certain studies indicated controversial results[10,11]. Using SBP recordings measured from finger plethysmography, we obtained low frequency power of SBP fluctuations. Briefly, SBP signals were re-sampled to 3.41 Hz (1024 points every 300 seconds) using cubic spline fitting; the power spectrum was obtained in each 2.5-minute window without gaps of data more than 5 seconds; and the average power spectrum was obtained from all 2.5-minute windows at baseline or during tilting for each cycle.

In addition to SBP LF power, we obtained high frequency power (HF; 0.15-0.5Hz) of SBP which has been suggested to reflect the effect of respiration[9]. Log scale LF (lnLF) and log scale HF (lnHF) were used in the analyses to ensure the normal distributions of the two variables.

In response to head-up tilt, there was a significant increase in lnLF of SBP (**Supplemental Figure V A**). This finding is consistent with the observation of increased plasma epinephrine and norepinphrine levels during head-up tilt (**Figures 4C** and **4D**), together indicating an increase in sympathetic activity during tilt. The lnLF change was not significant different between groups and between the trials with presyncope and without presyncope ($P > 0.1$). Similar to the change in epinephrine, the tilt-induced increase in lnLF of SBP showed a significant circadian rhythm with smaller increase during the biological night compared to the biological day (**Supplemental Figure VIA**), i.e., the increase was smallest at ~20^o (corresponding to 5:50AM) and largest at ~170^o (3:50PM). However, the circadian rhythm in the overall SBP lnLF (both conditions both groups) was not statistically significant.

lnHF of SBP also increased in response to head-up tilt (**Supplemental Figure V B**), suggesting increased respiratory effect during tilt compared to baseline. Mean lnHF and its

response to tilt showed no group differences and no differences between the 21 trials with presyncope and the 51 completed trials for the same presyncope group ($P > 0.1$). Moreover, mean lnHF and its response to tilt showed no significant rhythms (**Supplemental Figure VI B**).

Changes in cardiovascular variables throughout the head-up tilt test

Stable phase during head-up tilt. During the stable phase after tilt-up (1-minute period after ~1-minute tilt-up), there was a large decrease in stroke volume (SV) and a significant decrease in ejection time (EJT) for both presyncopal and non-presyncopal groups compared to baseline (Panels A and C of **Supplemental Figure X**). Cardiac output (CO) also decreased significantly but not dramatically as SV (**Supplemental Figure X B**) due to increased heart rate (HR) (Mean±SE: 85.5 ± 2.5; baseline 62.1 ± 2.5; $P < 0.0001$). Total peripheral resistance (TPR) increased at such initial stage of tilt as compared to baseline (**Supplemental Figure X D**). The decrease in CO and the increase in TPR were more pronounced in the presyncopal group, but the group difference was only significant in the TPR change (the group difference in the CO change did not reach significant level; $P = 0.06$). Changes of SV and EJT were not significantly different between groups. Within presyncope group, there were no differences in all four variables and their tilt-induced changes between aborted tests and completed tests.

The circadian pacemaker had a significant influence on CO, leading to a significant circadian rhythm ($P = 0.00039$) with the minimal CO at ~300^{o} (corresponding to ~10:30PM) that was consistent for both groups and during both baseline and tilt conditions (**Supplemental Figure XI B**). There was also a significant circadian rhythm in EJT but not in SV and TPR (**Supplemental Figure XI**). There were no interactions between tilt and circadian influences in the four variables. Though average CO was not significantly different between groups (**Supplemental Figure X B**), there was an interaction between circadian and group influences on CO (averaged

for baseline and tilt), i.e., presyncopal group generally had smaller CO and the group difference was much less at 300^{o}-360^{o} compared to other circadian phases (P = 0.037). We found no significant interactions between group and circadian influences on SV, EJT, and TPR.

At the end of head-up tilt. Before tilting down (10 seconds before putting the tilt table to the horizontal position), the non-presyncopal group showed no significant changes in SBP, DBP, SV, CO, and TPR, , as compared to initial stage of tilt-up (**Supplemental Figure XII**). There was a slight increase in HR (P = 0.016), and a slight decrease in EJT (P = 0.031). In contrast, the presyncopal group showed overall (including trials with and without presyncope) significant decreases in SBP (P <0.001), DBP (P <0.001), SV (P <0.001), and CO (P = 0.0023) before tilting down, but no significant changes in HR, EJT, and TPR.

Within the presyncopal group, the decreases in SBP (P <0.001) and SV (P = 0.048) were more pronounced during the presyncope trials while the decreases in DBP (P <0.001) and CO (P <0.001) were only pronounced during the presyncope trials. EJT decreased only in trials without presyncope in the presyncopal group (P = 0.04). Though mean HR and TPR in all presyncope trials showed no significant changes before tilting down, we noted that the behaviors of these variables could be different in the presence of presyncope, depending on the timing of aborting the tests (see "Presyncope during tilt-table testing" in the **Results** section of the main manuscript). For instance, HR might still remain increased if subjects were tilted down early/immediately when signs/symptoms of presyncope just appeared; or HR could start to decrease dramatically if tilting down occurred when syncope was almost fully developed (**Figure 2**). Such a dynamic effect may explain the large variations of the HR and TPR changes before being tilted down in the 21 presyncope trials (**Supplemental Figure XII**).

Supplemental Tables

Supplemental Table I. Specification of the generalized linear mixed model (GLMM) for the assessment of the circadian distribution of presyncope events. Test outcomes of all 12 subjects (12x12=144 tests) were pooled together for the analysis. Results are presented in Figure 3B of the main manuscript.

GLMM	Variable	Parameter Type
Response	Presyncope (Yes or No)	Binary
Fixed effect (s)	Circadian bin	Nominal
Random factor	Subject	Nominal

Supplemental Table II. Specification of the mixed models for the assessment of effects of tilt, group (presyncopal group: those with presyncope; non-presyncopal group: those who never experienced presyncope throughout the protocol), and their interactions on physiological variables. Standard least squares and restricted maximum likelihood methods were used for fitting mixed models. Data from the baseline and tilt conditions (in all 144 tests) were pooled together for the analysis. Results are presented in Figure 4 of the main manuscript.

Mixed-model ANOVA	Variable	Parameter type
Response	Physiological variable (e.g., SBP, DBP, and HR)	Continuous
Fixed effects	Condition (baseline or tilt) Group Condition*Group	Nominal Nominal Nominal
Random factor	Subject (nested in group)	Nominal

Supplemental Table III. Specification of the mixed models for the assessment of differences in baseline variables and their responses to tilt between trials with and without presyncope within the presyncopal group. Data of 6 subjects with presyncope experience (21 trials with presyncope and 51 without presyncope) during both the baseline and tilt conditions were pooled together for the analysis. Standard least squares and restricted maximum likelihood methods were used for fitting mixed models. Results are presented in Figure 5 of the main manuscript.

Mixed-model ANOVA	Variable	Parameter type
Response	Physiological variable (e.g., SBP and DBP)	Continuous
Fixed factors	Presyncope (yes or no) Condition (baseline or tilt) Condition*Presyncope	Nominal Nominal Nominal
Random factor	Subject	Nominal

Supplemental Table IV. Specification of the mixed models for the assessment of the effects of circadian phase and its interactions with tilt and group effects on physiological variables. θ is circadian phase determined from the core body temperature (see Supplemental Figures I-II). Data from both the baseline and tilt conditions from all 144 tests were pooled together for the analysis. Results are presented in Figure 6 and the Table of the main manuscript.

Mixed-model ANOVA	Name of variable or factor	Parameter Type
Response	Physiological variable (e.g., SBP, DBP)	Continuous
Fixed factors	*Intercept* *cosθ* *sinθ* *cos2θ* *sin2θ* Condition (baseline or tilt) Condition**cosθ* Condition**sinθ* Condition**cos2θ* Condition**sin2θ*	Continuous Continuous Continuous Continuous Continuous Nominal Continuous Continuous Continuous Continuous
Random factor	Subject	Nominal

Supp

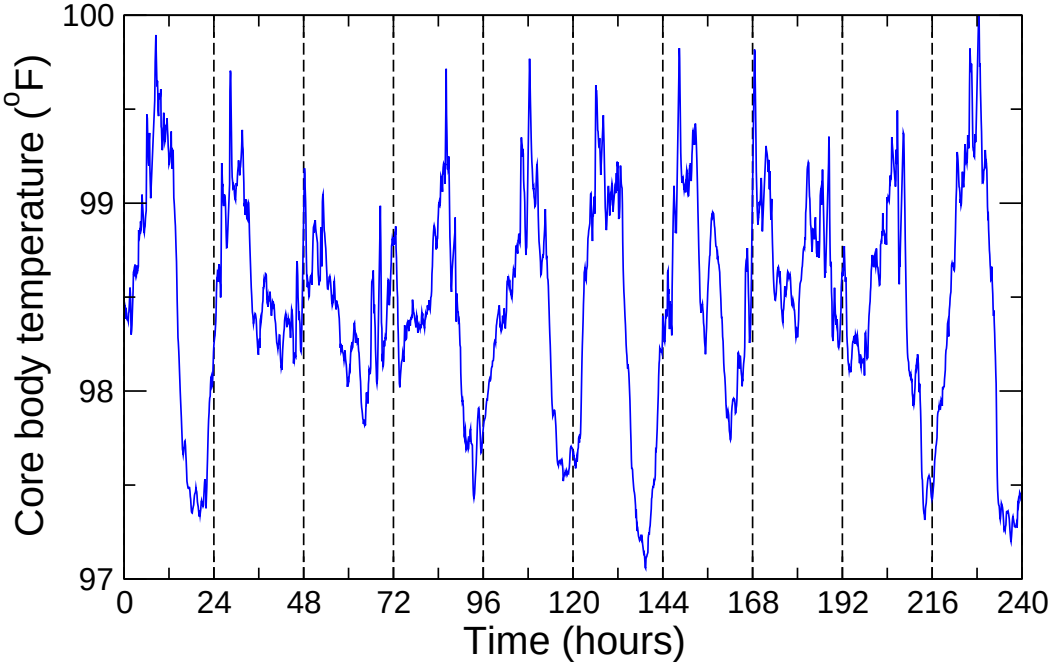

Supplemental Figure I. Core body temperature of one subject throughout the 10-day forced desynchrony phase (twelve 20-h cycles) in the experimental protocol.

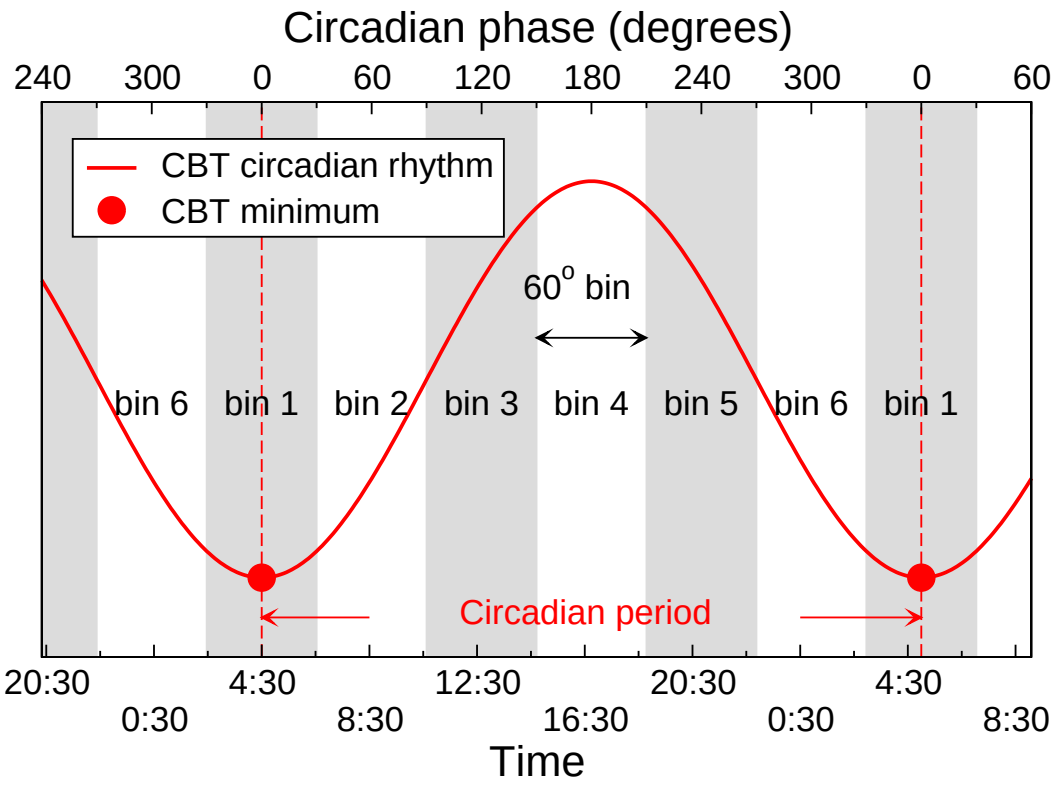

Supplemental Figure II. A schematic representation of circadian phase estimation and data binning. The phase, period (τ =~24 h) and amplitude of circadian oscillations were estimated from least squares regression of core body temperature recording throughout the entire study. Circadian phase was assigned as 0^{o} at the time of CBT minimum (t_{min}) and each data point was assigned a circadian phase, i.e., for a data point at time t <τ, the circadian phase = $360*(t- t_{min})/\tau$.

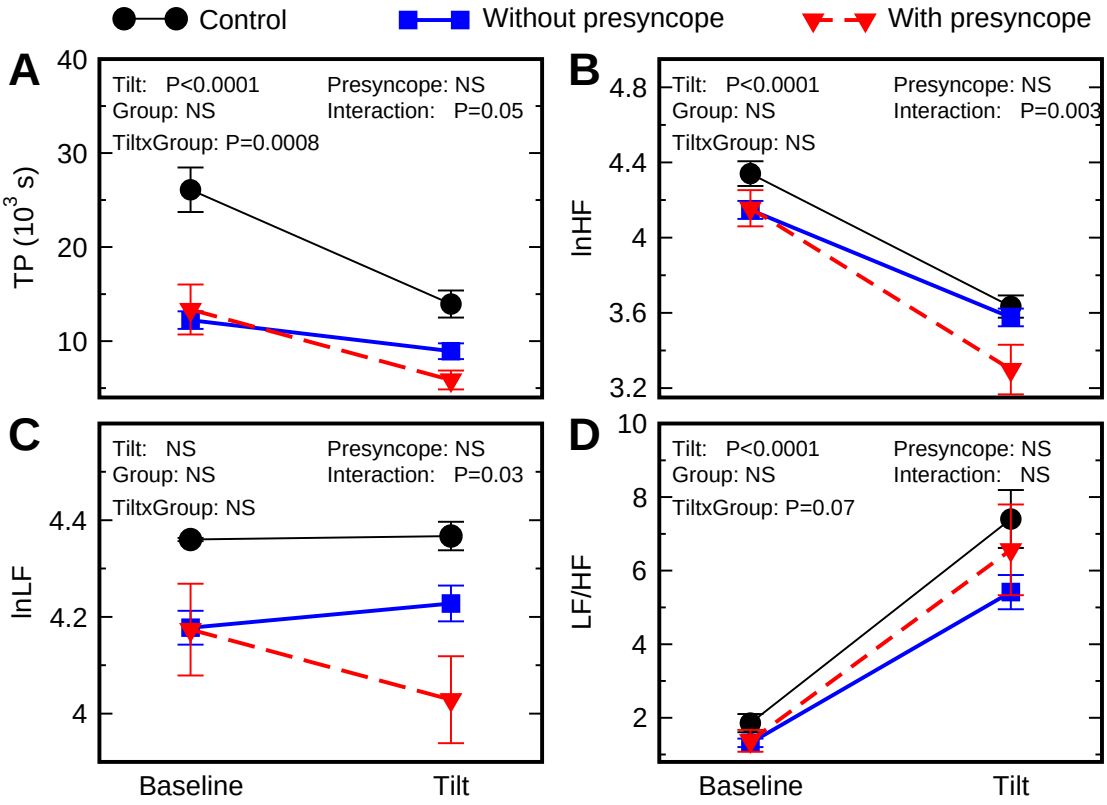

Supplemental Figure III. Responses of frequency-domain HRV indices to head-up tilt, and their differences between the non-presyncopal (black) and the presyncopal groups, and between completed trials (blue) and aborted trials (red) in the presyncopal group. Data are presented as mean±SE. Shown at the left corners of panels are P values for: (i) tilt effects (significant for all variables except for lnLF); (ii) mean group differences (P>0.1 for all variables); and (iii) the interaction between group and tilt stressor (only significant for TP). Also shown at the right corners of panels are P values for differences in (i) overall mean values (both baseline and tilt; P > 0.1 for all variables) and (ii) tilt responses (significant for lnLF and lnHF) between the 21 presyncope cases and the other 51 trials without presyncope within the presyncopal group. Results were obtained from the mixed models specified in **Supplemental Table II** for group comparisons and in **Supplemental Table III** for within-group comparisons. "NS" indicates not significant (here, P always >0.1).

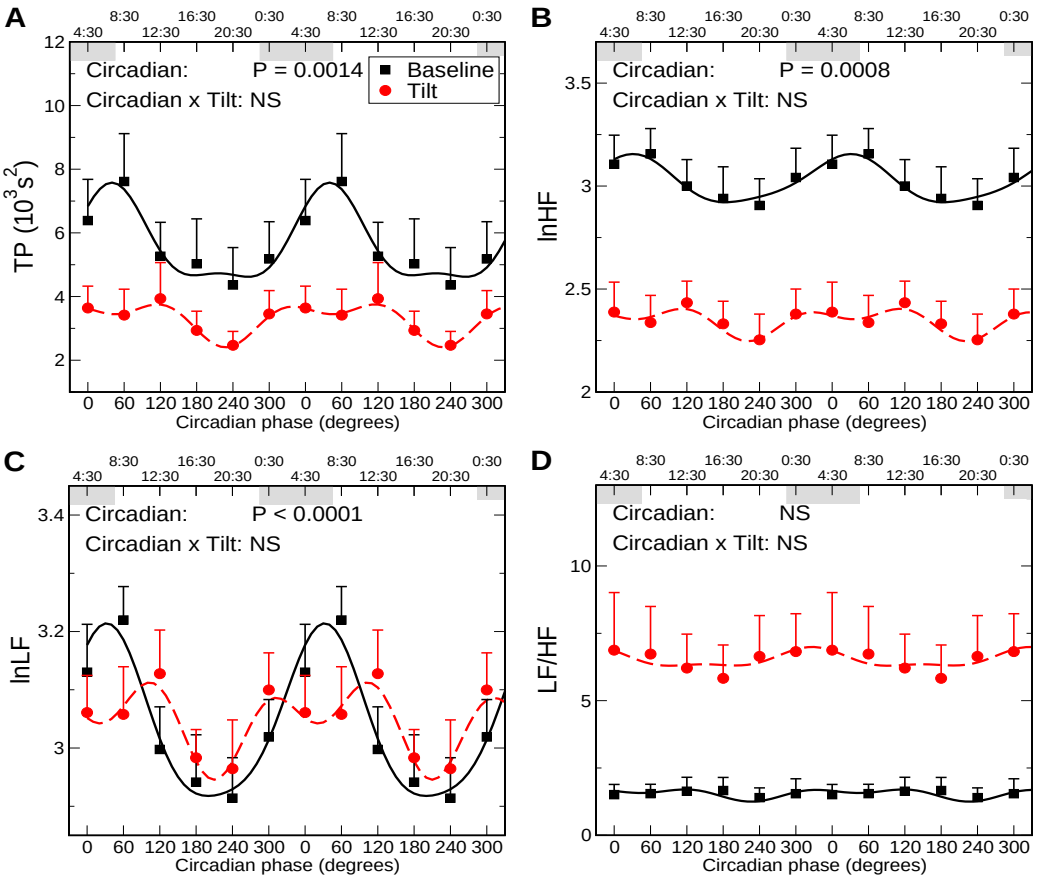

Supplemental Figure IV. Circadian influences on frequency-domain HRV indices and their responses to head-up tilt. The data (symbols) and the cosinor fits (lines) are plotted separately for baseline (black squares and continuous lines) and head-up tilt (circles and dashed lines). Gray bars indicate the average habitual sleep period when living outside of the laboratory. The data are presented as mean±SE across subjects. The results are double plotted to better visualize rhythmicity, with circadian phase on the lower abscissa and the corresponding habitual time of day on the upper abscissa. Shown are the mixed model derived P values for circadian influences (significant for TP, lnLF and lnHF) and interaction between tilt and circadian influences (not significant for all variables). There were no significant interactions between circadian and group effects for all variables. "NS" indicates not significant (here, P always >0.1). Results were obtained from the cosinor analyses using mixed-model ANOVAs (**Supplemental Table IV**).

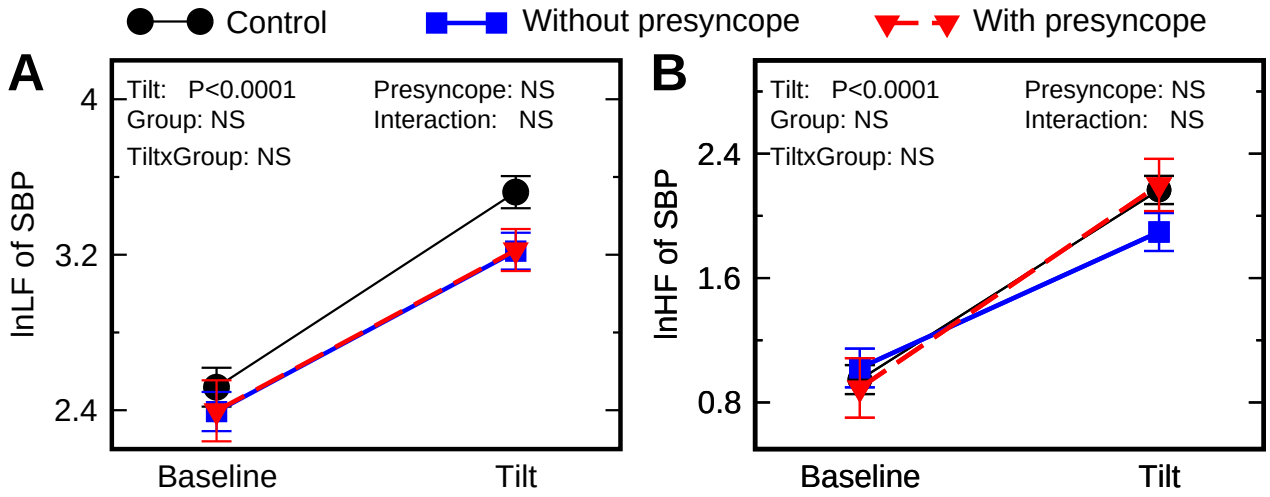

Supplemental Figure V. Responses of low and high frequency powers of systolic blood pressure (SBP) fluctuations to head-up tilt, and their differences between the non-presyncopal (black) and the presyncopal groups, and between completed trials (blue) and aborted trials (red) in the presyncopal group. Log scales of low frequency (lnLF) and high frequency (lnHF) were used and data are presented as mean±SE. Shown at the left corners of panels are P values for: (i) tilt effects (significant for both lnLF and lnHF); (ii) mean group differences (P>0.1 for both variables); and (iii) the interaction between group and tilt stressor (P > 0.1 for both variables). Within the presyncopal group, lnHF and lnLF were not significantly different between the 21 presyncope cases and the other 51 trials without presyncope. "NS" indicates not significant (here, P always >0.1). Results were obtained from the mixed models specified in **Supplemental Table II** for group comparisons and in **Supplemental Table III** for within-group comparisons.

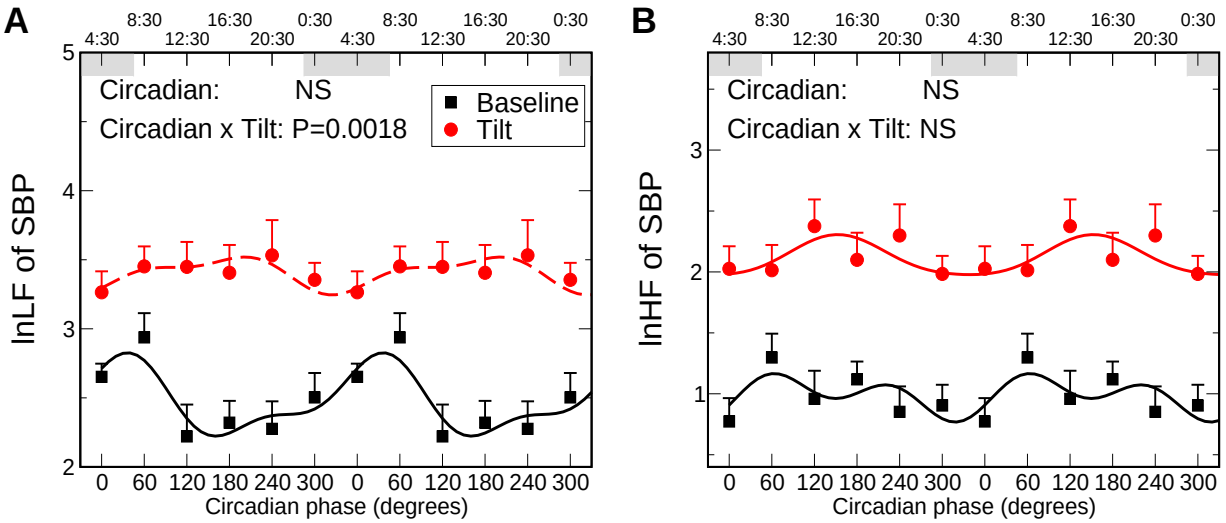

Supplemental Figure VI. Log scales of low and high frequency powers of systolic blood pressure at different circadian phases. The data (symbols) and the cosinor fits (lines) are plotted separately for baseline (black squares and continuous lines) and head-up tilt (circles and dashed lines). Gray bars indicate the average habitual sleep period when living outside of the laboratory. The data are presented as mean±SE across subjects. The results are double plotted to better visualize rhythmicity, with circadian phase on the lower abscissa and the corresponding habitual time of day on the upper abscissa. Shown are the mixed model derived P values for circadian influences (not significant for both lnLF and lnHF) and interaction between tilt and circadian influences (significant for lnLF). There were no significant interactions between circadian and group effects on both variables. Results were obtained from the cosinor analyses using mixed-model ANOVAs (**Supplemental Table IV**).

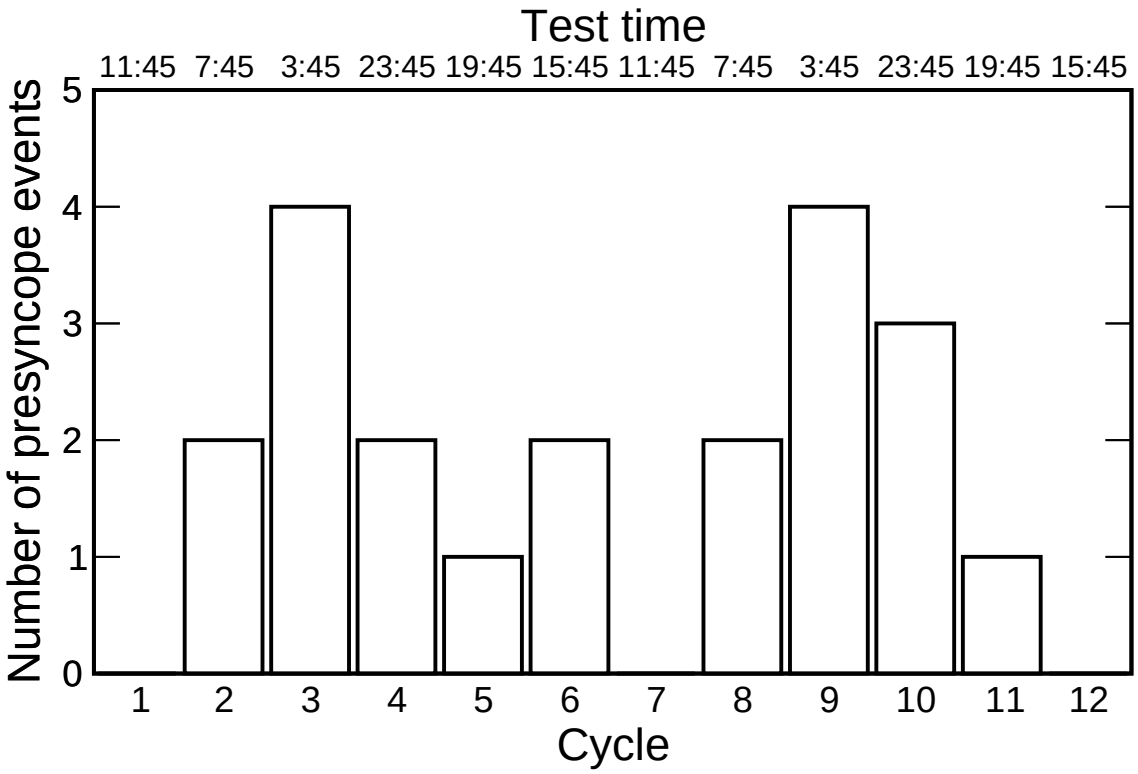

Supplemental Figure VII. Distribution of presyncope events across 12 sequential 20-h cycles throughout the forced desynchrony protocol. There were 11 presyncope events during the first 6 cycles and 10 during the last 6 cycles, thus there was no simple systematic effect of time into the protocol on incidence of presyncope, except for a clear underlying endogenous circadian rhythm indicated by two clear peaks in the frequency of presyncope events at Cycle 3 and Cycle 9 when the head-up tilt tests were performed during the biological night (the corresponding circadian phase bin of 180°). The upper abscissa of the figure is the average time of day (for the 6 presyncopal subjects) when head-up tilt tests were performed.

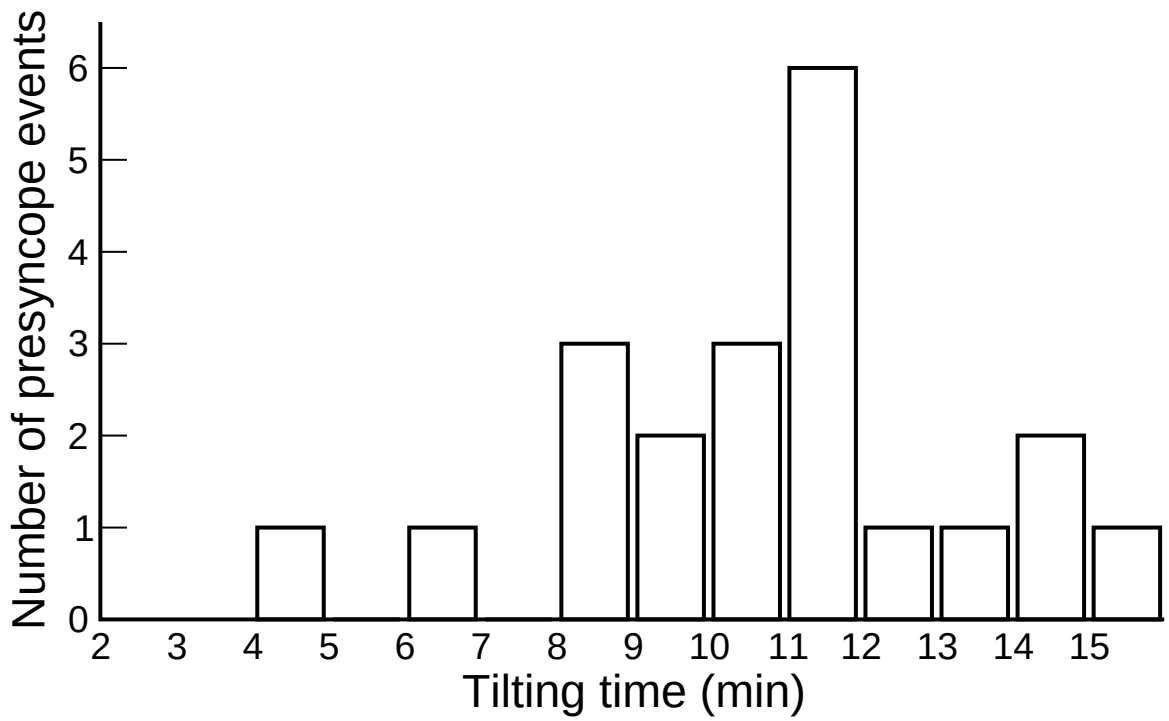

Supplemental Figure VIII. Distribution of tilt duration in 21 head-up tilt tests with presyncope. Most of presyncope events occur between 8-12 minutes after being tilted up.

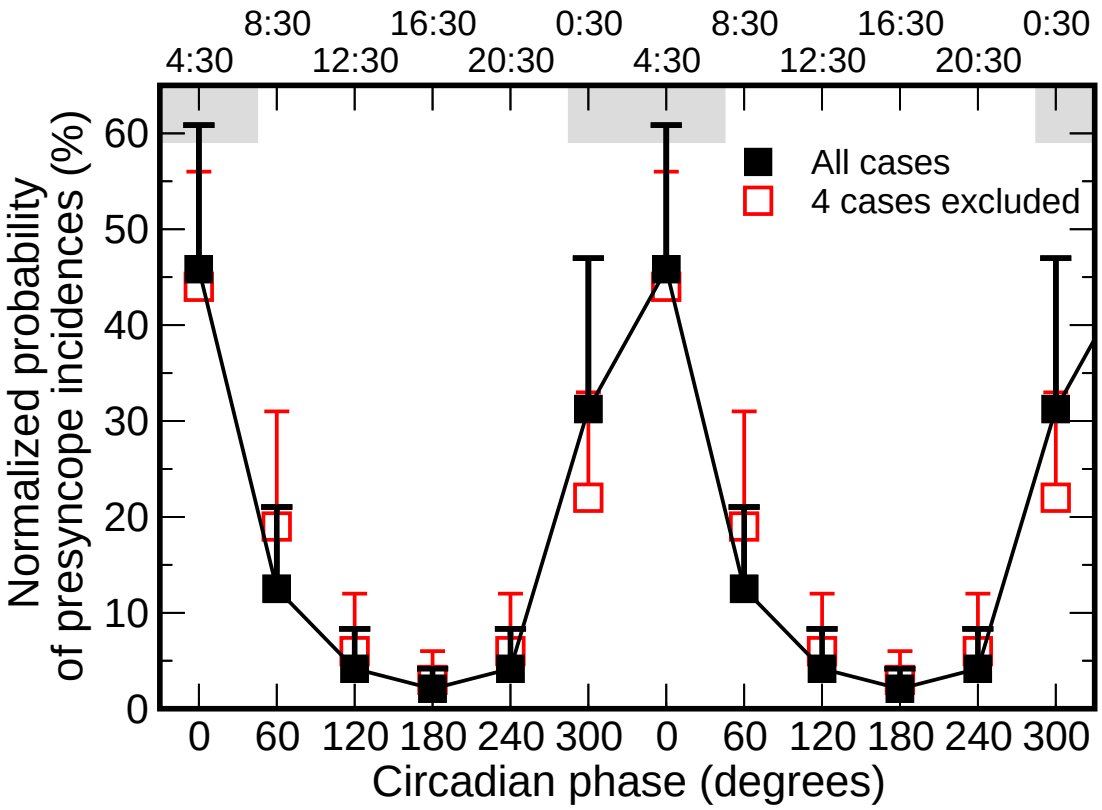

Supplemental Figure IX. Average probability of presyncope occurrence across all circadian phases. Gray bars indicate the average habitual sleep period when living outside of the laboratory. Error bars are standard errors. Results were double plotted to better visualize rhythmicity, with circadian phase on the lower abscissa and the corresponding habitual time of day on the upper abscissa. A generalized linear mixed model revealed significant level of circadian influence when including all 21 presyncope cases ($P = 0.028$). A similar circadian variation was observed ($P = 0.042$) when excluding 4 presyncope cases when tests were aborted mainly due to symptoms without significant hypotension (assigning the 4 cases as completed trials).

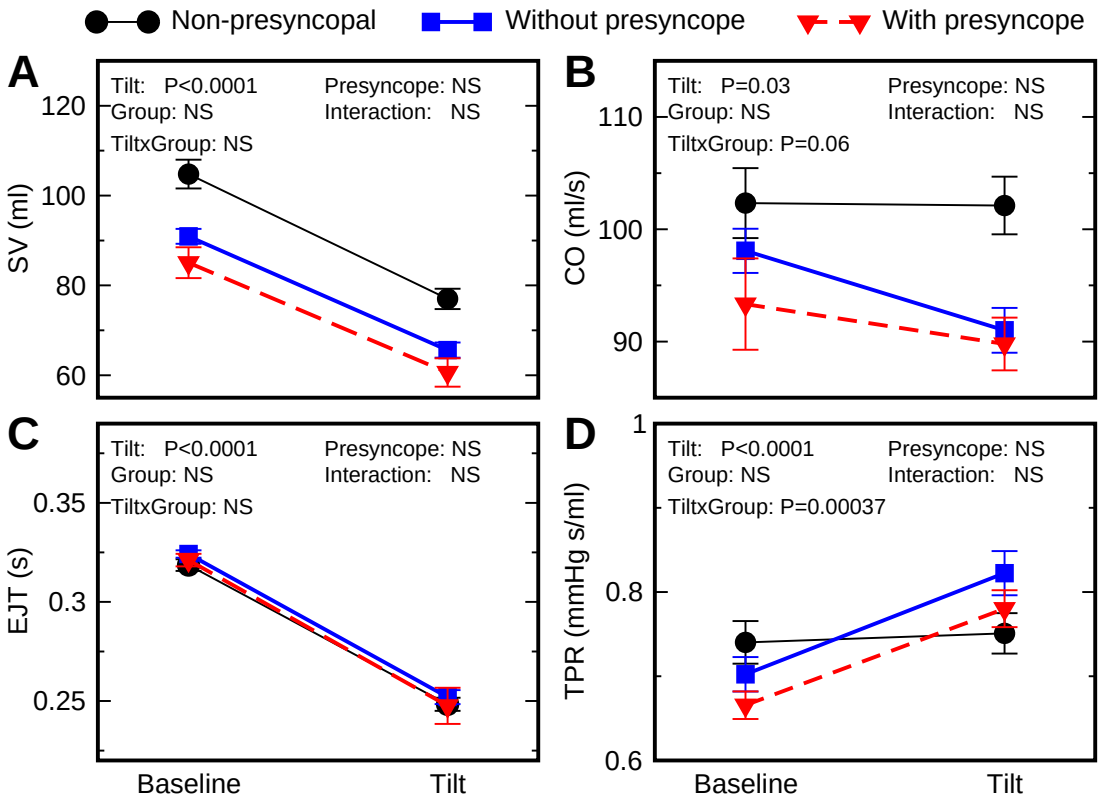

Supplemental Figure X. Responses of stroke volume (SV), cardiac output (CO), ejection time (EJT) and total peripheral resistance (TPR) to head-up tilt, and their differences between the non-presyncopal (black) and the presyncopal groups, and between completed trials (blue) and aborted trials (red) in the presyncopal group. Results were obtained from finger plethysmography and data are presented as mean±SE. Shown at the left corners of panels are P values for: (i) tilt effects (significant for all variables); (ii) mean group differences (P>0.1 for all variables); and (iii) the interaction between group and tilt stressor (significant forTPR). Within the presyncopal group, all these four variables and their responses to tilt were not significantly different between the 21 presyncope cases and the other 51 trials without presyncope (as shown by "NS" shown at right corners). Results were obtained from the mixed models specified in **Supplemental Table II** for group comparisons and in **Supplemental Table III** for within-group comparisons. "NS" indicates not significant (here, P always >0.1).

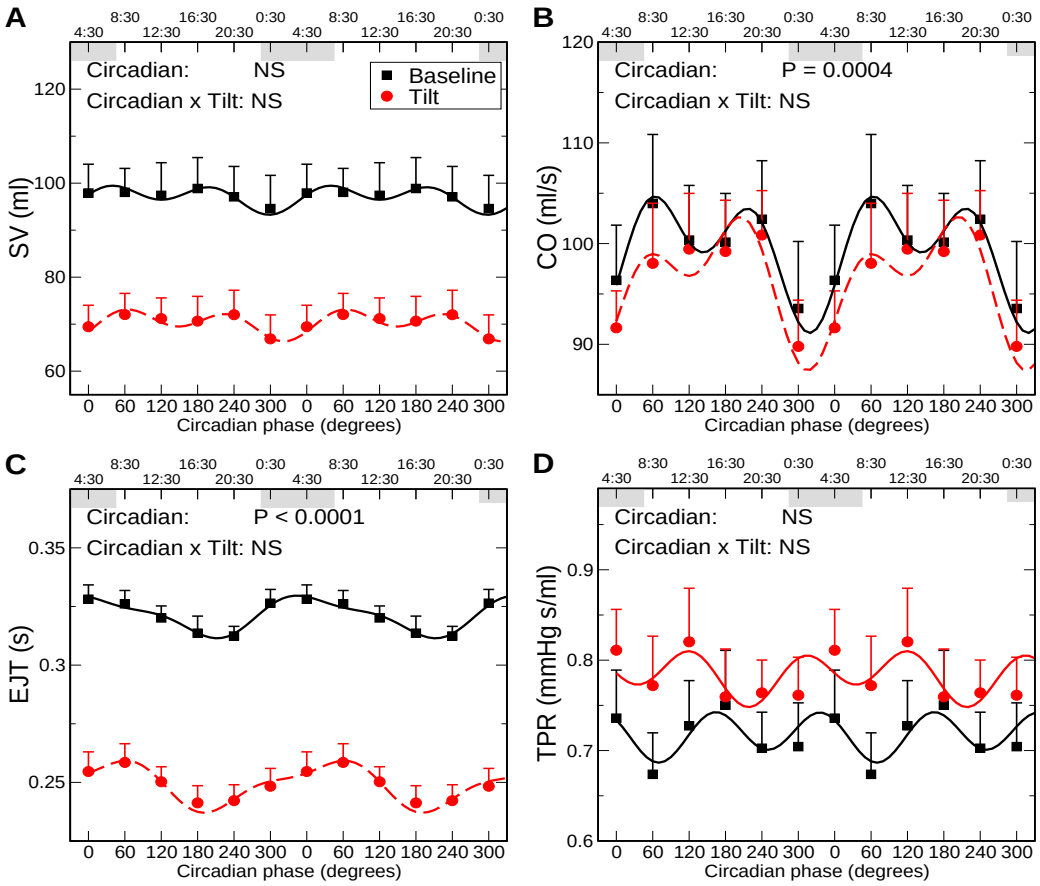

Supplemental Figure XI. Circadian influences on stroke volume (SV), cardiac output (CO), ejection time (EJT) and total peripheral resistance (TPR), and their responses to head-up tilt. The data (symbols) and the cosinor fits (lines) are plotted separately for baseline (black squares and continuous lines) and head-up tilt (circles and dashed lines). Gray bars indicate the average habitual sleep period when living outside of the laboratory. The data are presented as mean±SE across subjects. The results are double plotted to better visualize rhythmicity, with circadian phase on the lower abscissa and the corresponding habitual time of day on the upper abscissa. Shown are the mixed model derived P values for circadian influences (significant for CO and EJT). There was no significant interaction between tilt stressor and circadian phase for any of these variables. Results were obtained from the cosinor analyses using mixed-model ANOVAs (**Supplemental Table IV**).

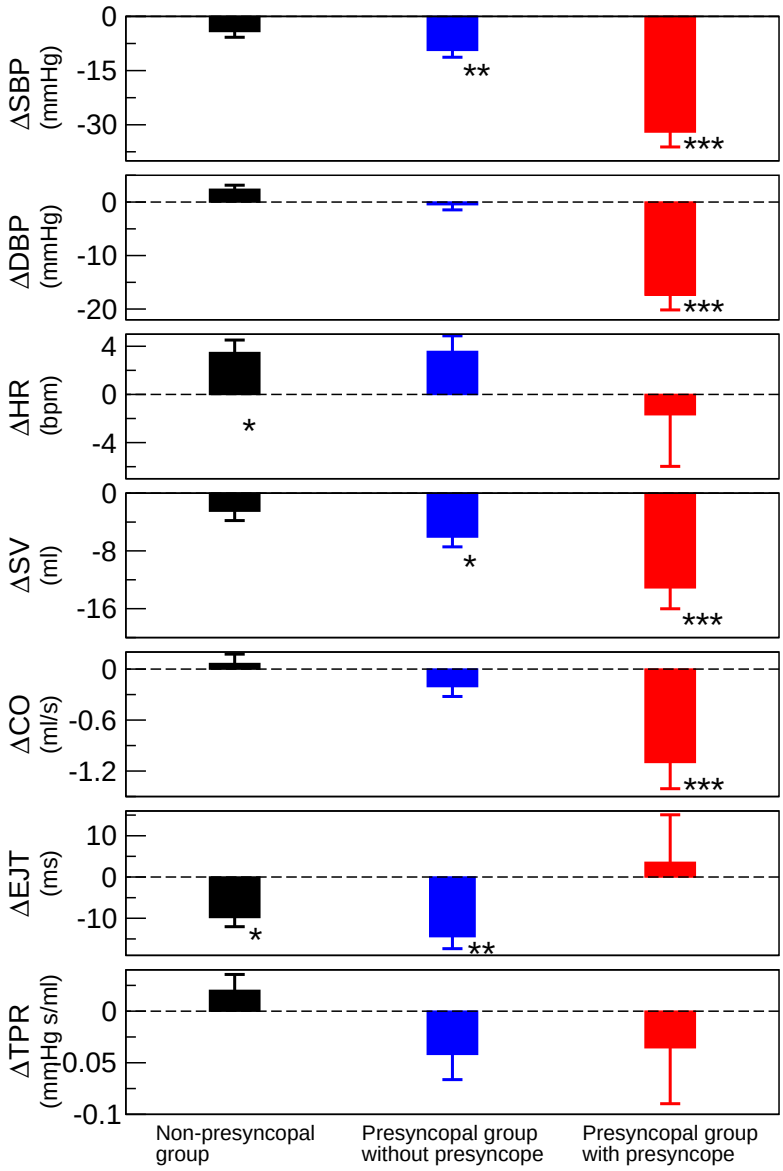

Supplemental Figure XII. Changes in physiological variables at the end of head-up tilt as compared to at the initial stable phase of tilt. Shown are the changes between 10 seconds before being tilted down and ~1 minute after being tilted up in systolic blood pressure (ΔSBP), diastolic blood pressure (ΔDBP), heart rate (ΔHR), stroke volume (ΔSV), cardiac output (ΔCO), ejection time (ΔEJT) and total peripheral resistance (ΔTPR). Significant changes are indicated by *($P < 0.05$), **($P < 0.001$), and ***($P<0.0001$). Results were obtained from the mixed model ANOVAs in which subject was included as a random effect for intercept.

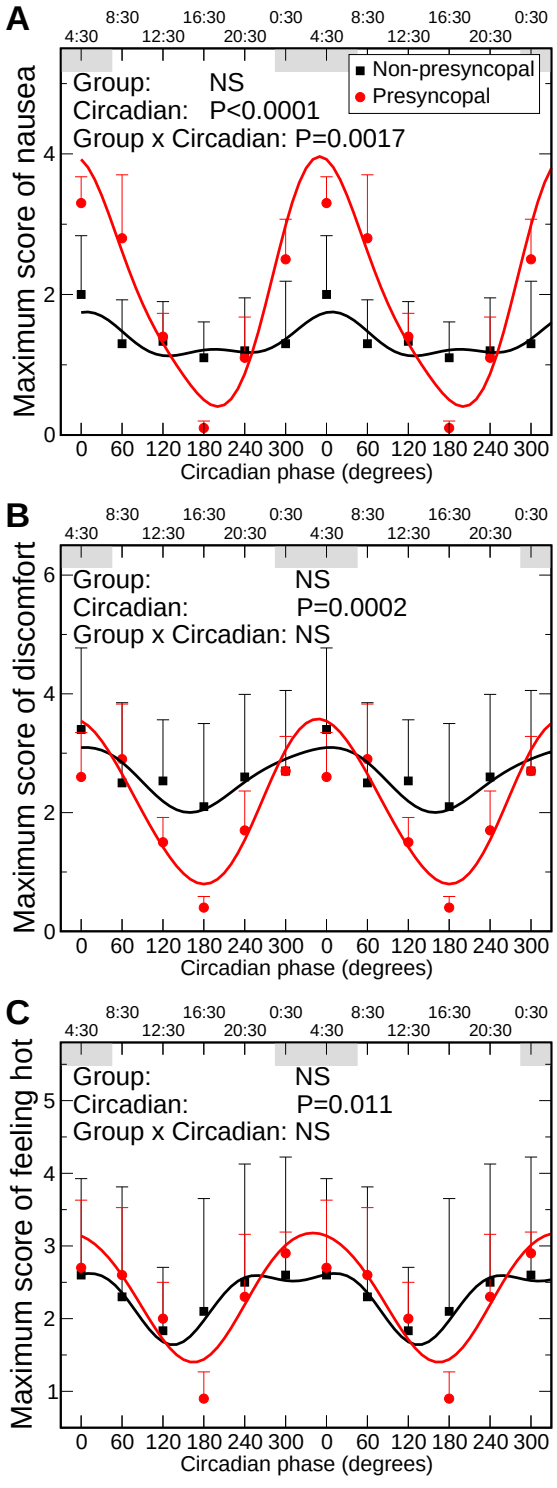

Figure XIII. Endogenous circadian rhythms in subjective scores of **A**. "nausea", **B**. "general discomfort", and **C**. "feeling hot" during tilt-testing. The binned data (symbols) and the cosinor model fits (lines) were plotted separately for the non-presyncopal group (squares and lines) and the presyncopal group (circles and lines). Gray bars indicate the average habitual sleep period when living outside of the laboratory. Data are presented as mean±SE across subjects. The results are double plotted to better visualize rhythmicity, with circadian phase on the lower abscissa and the corresponding habitual time of day on the upper abscissa. Shown are the mixed model derived P values for: (i) group differences (not significant or "NS" for all variables); (ii) circadian influences (significant for all variables); and (iii) interaction between group and circadian phase (significant for the nausea score). Results were obtained from the cosinor analyses using mixed-model ANOVAs in which effects of group, circadian and their interaction were included as fixed effects and subject was as a random factor for intercept.

Supplemental References

1. Czeisler CA, Duffy JF, Shanahan TL, Brown EN, Mitchell JF, Rimmer DW, Ronda JM, Silva EJ, Allan JS, Emens JS, Dijk DJ, Kronauer RE. Stability, precision, and near-24-hour period of the human circadian pacemaker. *Science*. 1999;284:2177-2181.

2. Halberg F, Tong YL, Johnson EA. Circadian system phase—an aspect of temporal morphology. In: von Mayersbach H, editor. The Cellular Aspects of Biorhythms. Berlin: Springer, 1967: 20-48.

3. Nelson W, Tong YL, Lee JK, Halberg F. Methods for cosinor-rhythmometry. *Chronobiologia*. 1979;6:305-323.

4. Tong YL. Parameter estimation in studying circadian rhythms. *Biometrics*. 1976;32:85-94.

5. Mikulich SK, Zerbe GO, Jones RH, Crowley TJ. Comparing linear and nonlinear mixed model approaches to cosinor analysis. *Stat Med*. 2003;22:3195-3211.

6. Heart rate variability: standards of measurement, physiological interpretation and clinical use. Task Force of the European Society of Cardiology and the North American Society of Pacing and Electrophysiology. *Circulation*. 1996;93:1043-1065.

7. Pagani M, Lucini D, Rimoldi O, Furlan R, Piazza S, Porta A, Malliani A. Low and high frequency components of blood pressure variability. *Ann N Y Acad Sci*. 1996;783:10-23.

8. Pagani M, Montano N, Porta A, Malliani A, Abboud FM, Birkett C, Somers VK. Relationship between spectral components of cardiovascular variabilities and direct measures of muscle sympathetic nerve activity in humans. *Circulation*. 1997;95:1441-1448.

9. Brychta RJ, Shiavi R, Robertson D, Biaggioni I, Diedrich A. A simplified two-component model of blood pressure fluctuation. *Am J Physiol Heart Circ Physiol*. 2007;292:H1193-H1203.

10. Taylor JA, Williams TD, Seals DR, Davy KP. Low-frequency arterial pressure fluctuations do not reflect sympathetic outflow: gender and age differences. *Am J Physiol*. 1998;274:H1194-H1201.

11. Myers CW, Cohen MA, Eckberg DL, Taylor JA. A model for the genesis of arterial pressure Mayer waves from heart rate and sympathetic activity. *Auton Neurosci*. 2001;91:62-75.